

Significant Enhancement of Energy Barriers in Dinuclear Dysprosium Single-Molecule Magnets Through Electron-Withdrawing Effects

Fatemah Habib,[†] Gabriel Brunet,[†] Veacheslav Vieru,[‡] Ilia Korobkov,[†] Liviu F. Chibotaru,[‡] and Muralee Murugesu^{*†}

[†]Chemistry Department, University of Ottawa, 10 Marie Curie, Ottawa, ON, K1N6N5, Canada

[‡]Division of Quantum and Physical Chemistry and INPAC–Institute for Nanoscale Physics and Chemistry, Katholieke Universiteit Leuven, Celestijnenlaan, 200F, 3001, Belgium

S Supporting Information

ABSTRACT: The effect of electron-withdrawing ligands on the energy barriers of Single-Molecule Magnets (SMMs) is investigated. By introducing highly electron-withdrawing atoms on targeted ligands, the energy barrier was significantly enhanced. The structural and magnetic properties of five novel SMMs based on a dinuclear $\{Dy_2\}$ phenoxo-bridged motif are explored and compared with a previously studied $\{Dy_2\}$ SMM (1). All complexes share the formula $[Dy_2(\text{valdien})_2(L)_2]\cdot\text{solvent}$, where $H_2\text{valdien} = N1,N3\text{-bis}(3\text{-methoxysalicylidene})\text{ diethylenetriamine}$, the terminal ligand $L = NO_3^-$ (1), CH_3COO^- (2), $C1CH_2COO^-$ (3), $C1_2CHCOO^-$ (4), $CH_3COCHCOCH_3^-$ (5), $CF_3COCHCOCF_3^-$ (6), and solvent = 0.5 MeOH (4), 2 CH_2Cl_2 (5). Systematic increase of the barrier was observed for all complexes with the most drastic increase seen in 6 when the acac ligand of 5 was fluorinated resulting in a 7-fold enhancement of the anisotropic barrier. *Ab initio* calculations reveal more axial g tensors as well as higher energy first excited Kramers doublets in 4 and 6 leading to higher energy barriers for those complexes.

The push to miniaturize devices in the nanotechnology world, including memory storage and other spintronic devices,¹ has led to the persistent investigation of $4f$ lanthanide elements as magnetic centers.² Their highly anisotropic nature has certainly been advantageous when targeting magnetic materials on a molecular level.³ Furthermore, they have been at the forefront of major advances in the field of Single-Molecule Magnets (SMMs) yielding higher effective energy barriers for spin reversal and the highest blocking temperatures to date.⁴ While the energy barriers (which result in magnetic bistability and slow magnetization relaxation) have been steadily increasing with different molecular clusters, a more systematic approach is required in order to elucidate the origin of slow relaxation as well as target rational methods of synthesizing better SMMs. As a point of reference, we based our study on a previously published $\{Dy_2\}$ SMM with terminal nitrate anionic ligands (complex 1, Figure 1).⁵ This well-studied complex exhibits an effective anisotropic barrier for the reversal of the magnetization of $U_{\text{eff}} = 76$ K. By substituting the nitrate terminal ligands with other bidentate, monoanionic ligands with varying electron-withdrawing substituents, we intend to study

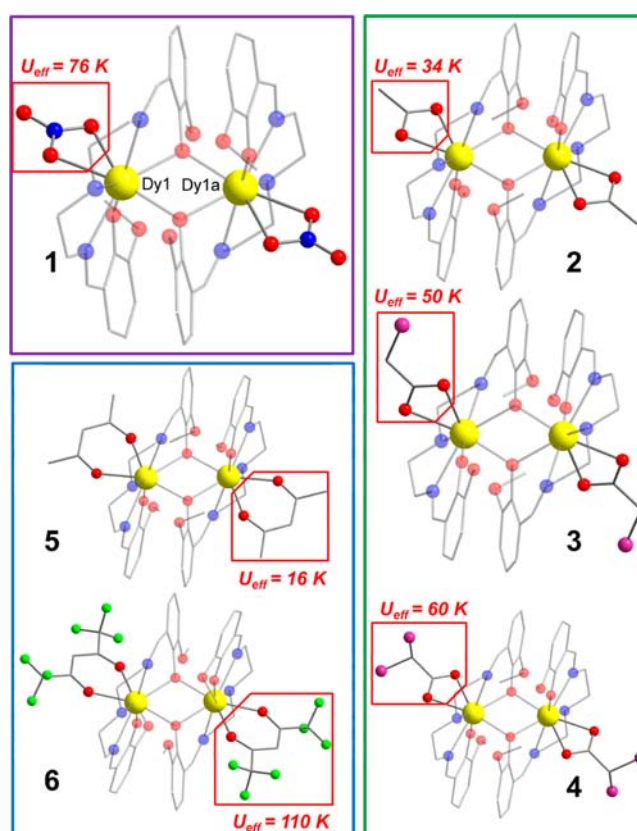


Figure 1. Molecular structures of complexes 1–6 highlighting the difference in terminal ligands (red boxes). The effective energy barriers (U_{eff}) are indicated. Color code: yellow (Dy), red (O), blue (N), gray (C), maroon (Cl), green (F).

the effects on the anisotropic barriers of the $\{Dy_2\}$ complexes. To the best of our knowledge, a direct correlation between relaxation barriers and electron-withdrawing groups on terminal ligands while maintaining the geometry of the lanthanide ions has never been previously reported. Herein we report the effects of electron-withdrawing substituents on the enhancement of the energy barriers for five novel $\{Dy_2\}$ SMMs.

Received: May 14, 2013

Published: August 21, 2013

The reaction of Dy(III) precursor with the ligand, *N*1,*N*3-*bis*(3-methoxysalicylidene)diethylenetriamine (*H*₂valdien) and the applicable terminal ligand (Figure 1, red boxes) under basic conditions yielded complexes 1–6 with the general formula [Dy₂(valdien)₂(L)₂].solvent, where the terminal ligand L = NO₃[−] (1), CH₃COO[−] (2), ClCH₂COO[−] (3), Cl₂CHCOO[−] (4), CH₃COCHCOCH₃[−] (acac, 5), CF₃COCHCOCF₃[−] (F₆acac, 6) and solvent = 0.5 MeOH (4), 2 CH₂Cl₂ (5) (Figure 1). The synthetic procedures as well as detailed crystallographic data are discussed in the ESI and Table S1. All six complexes are centrosymmetric and share the same dinuclear core structure; they consist of two Dy(III) metal ions, two dianionic tetradentate valdien ligands, and two bidentate monoanionic terminal ligands. A fully labeled molecular structure of 2 is presented in Figure S1, all other complexes follow the same labeling scheme. Additionally, the closest intermolecular distances between Dy(III) ions were found to be 7.36 (1), 7.62 (2), 7.68 (3), 7.82 (4), 9.79 (5), and 9.28 Å (6) indicating well-isolated units. In recent years, many studies have been undertaken to determine the effects of geometry changes on the slow relaxation of magnetic ions and subsequently on the energy barriers for reversal of the magnetization, especially for lanthanide ions.^{6,7} However, studies of systematic electronic changes while maintaining the coordination geometry of the metal centers have yet to be explored. In order to accurately postulate a relationship between the electronics of a system and the slow magnetization relaxation, our well-studied complex, 1, can be an ideal model. By sequentially modifying the monoanionic ligands while keeping the core of 1, the parent compound, we have developed two systems: complexes 2, 3, and 4 form one system, while the second comprises complexes 5 and 6. In both cases, the electron density on the coordinating oxygen atoms (O5 and O6) has been decreased by adding electron-withdrawing Cl (first system) or F atoms (second system) which renders the oxygen atoms significantly electron deficient (*vide infra* for *ab initio* calculations).

In order to probe the magnetic behavior of 2–6, direct current (dc) magnetic susceptibility measurements (Figure S2) indicate room temperature χT values of 28.85 (2), 27.52 (3), 27.76 (4), 27.84 (5), and 29.02 cm³·K·mol^{−1} (6), all of which are within reasonable agreement of the theoretical χT value for two noninteracting Dy(III) ions (⁶H_{15/2}, *S* = 5/2, *L* = 5, *g* = 4/3, *C* = 14.17 cm³·K·mol^{−1}). As the temperature decreases, the χT values remain relatively constant down to ~30 K for 2, 5, and 6 before rapidly dropping to a value of 10.4 (2.5 K, 2), 10.87 (1.8 K, 5) and 7.16 cm³·K·mol^{−1} (1.8 K, 6). For 3 and 4, the χT curve decreases steadily below 150 K before rapidly decreasing below 30 K reaching 4.85 and 4.94 cm³·K·mol^{−1} for 3 and 4, respectively, at 1.8 K. This observed behavior for 2–6 mirrors that of 1 which has been extensively studied and exhibits weak intramolecular antiferromagnetic interactions as well as significant magnetoanisotropy, both of which contribute to the decrease in the χT product. *Ab initio* calculations of the CASSCF/RASSI/SINGLE_ANISO type were carried out with MOLCAS 7.8 (Table S3) in order to simulate the static magnetic behavior for all complexes.⁸ The experimental magnetic data were reproduced well with antiferromagnetic interactions that were found to be highest for 4 in the first system and for 6 in the second system (Table S4, Figures S3–S7). The magnetization (*M*) plots as a function of field (*H*) and reduced field (*HT*^{−1}, Figure S8–S12) do not saturate nor superimpose on a single master curve confirming the presence

of anisotropy in all complexes. It is noteworthy that the curves at 1.8 K in the aforementioned plots show slight S-shape which has been previously attributed to intramolecular interactions.⁹

As mentioned above, the magnetic behavior of the parent compound, 1, has been studied using a variety of techniques including theoretical *ab initio* calculations and doping studies which investigated the intramolecular exchange biased interactions between Dy(III) centers.^{5a} In the present case, the effects of electronic changes to the monoanionic ligands on the slow magnetization relaxation are under study and can be probed using alternating current (ac) magnetic susceptibility measurements. The ac plots indicate frequency and temperature dependence of the in-phase (χ' , Figures S13, S14) and out-of-phase (χ'' , Figures 2, S15) susceptibilities confirming the

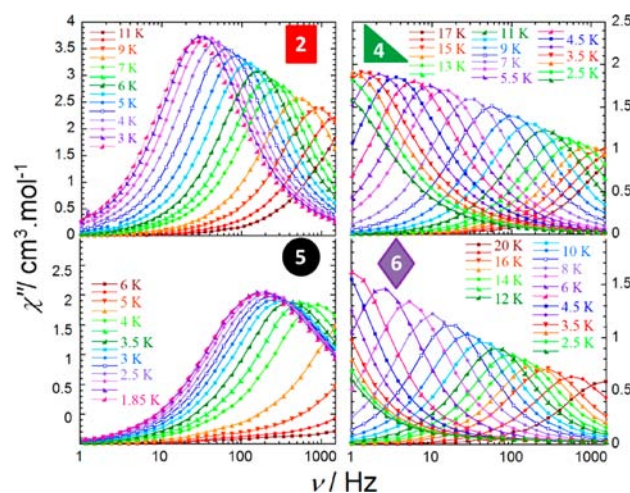


Figure 2. Selected frequency (ν) dependent out-of-phase magnetic susceptibility (χ'') plots for complexes 2, 4–6 at the indicated temperature ranges under zero applied dc field.

zero-field slow magnetization relaxation and SMM behavior of complexes 2–6. The presence of one relaxation process is attributed to the presence of one crystallographically independent Dy(III) ion in the centrosymmetric complexes.^{5a,10} The thermally induced relaxation can be fit using the Arrhenius law ($\tau = \tau_0 \exp(U_{\text{eff}}/kT)$) yielding effective energy barriers of $U_{\text{eff}} = 34$ (2), 50 (3), 60 (4), 16 (5), and 110 K (6). The Cole–Cole plots¹¹ for all complexes are shown in Figures S16–S20 and have been fit using a generalized Debye model. The α values are <0.05 in the higher temperature regions for 2–4 and 6, indicating the presence of a single relaxation mechanism. For 5, the α values are <0.25 which indicates a relatively narrow width of relaxation processes most likely due to a combination of QTM and thermally assisted relaxation pathways.

In deriving magneto-structural correlations, it is essential to look at the two systems separately. In order to provide a quantifiable structural comparison of the coordination spheres in complexes 1–6, the shape-measure approach was utilized based on the dihedral angles along the edges of the polyhedron of Dy1 (Figure S21, eq S1).¹² The parent complex, 1, was chosen as the reference polyhedron, and all other complexes were compared to it (Table S5). Within each system, the complexes were found to be analogous with a total deviation of <1.0° between 2–4 and 5–6. For 2–4 (first system), the difference in the structures corresponds to coordinating bidentate acetate groups (2), chloroacetate (3), and dichloro-

oacetate (4). The sequential addition of Cl atoms serves to withdraw electron density in a controlled fashion away from the coordinating oxygen atoms and, by extension, from the Dy–O5/O6 bonds (important bond distances and angles are presented in Table S2). The calculated electron density on the coordinating oxygen atoms of the terminal ligands using *ab initio* methods is shown in Table S6 and corresponds to an average decrease in electron density on O5/O6 as electron-withdrawing atoms are added. This leads to an increase in the corresponding Dy–O bond lengths (Table S2) and induces a stronger chemical bonding between Dy and O3/O3a, which is reflected in their shorter bond lengths (Table S2).¹³ This leads to a steady increase of the energy barrier in the first system from 34 K (2) to 50 K (3) to 60 K (4) and in the second system from 16 K (5) to 110 K (6) when the acac ligand is fluorinated. The electron-withdrawing ability of the hexafluoroacac ligand is much more significant (in 6, the average Dy–O_{terminal ligand} distance is longer by 0.07 Å, and the average charge on O5/O6 decreases by 0.087, Table S6) which translates into a more drastic increase in U_{eff} . The χ'' vs ν plots in Figure 2 also give an indication of the increase in the energy barrier; when U_{eff} increases, the frequency-dependent curves at different temperatures will span a much greater range of frequencies without reaching the QTM regime (where the peaks become temperature independent and begin to overlap) until very low ν as seen for 4 and 6. The χ'' vs ν plot for 3 is presented in Figure S15 and appears to span a wider range of frequencies than 2 but not quite as much as 4, in line with the intermediate U_{eff} of 50 K. The decrease in peak intensities as the temperature decreases to ~ 2 K is indicative of weak intramolecular interactions which were studied in the parent compound, 1.

A comparison of the relaxation times for complexes 1–6 with the average charge on coordinating oxygen atoms of the terminal ligands (Figure 3) indicates a correlation for these dinuclear Dy(III) systems. The more electron deficient the monoanionic bidentate terminal ligand, the higher the energy barrier of the $\{\text{Dy}_2\}$. From the Arrhenius plot, $\ln(\tau)$ vs T^{-1} , it is clear that the slope of the fit lines (at higher temperatures where thermal relaxation is dominant) become steeper as the coordinating oxygen atoms of the terminal ligands become more electron deficient leading to higher barriers (up to 110 K for the F_6acac -coordinated complex, 6). The large difference in the slow magnetization relaxation can be attributed to two reasons, outlined hereafter. The first is mainly due to the change in ligand field around the primary coordination sphere of the Dy(III) ions. The increased bond distance between the terminal ligand and the Dy(III) centers indicates a weaker bond which in turn supports the argument for a weaker ligand field acting on Dy(III). As the Dy–O_{terminal ligand} distance increases in 2–4 by adding electronegative atoms, the total splitting of the ground multiplet $^6\text{H}_{15/2}$ increases (Tables S7 and S8). However, for complexes 5 and 6, the first excited state of 6 decreased in energy significantly leading to greater mixing by spin–orbit coupling. The crystal field splitting becomes larger for 3, 4, and 6 in comparison to the nonhalogenated $\{\text{Dy}_2\}$ compounds with the calculated first spin–orbit multiplets in 4 and 6, being indeed higher in energy in comparison to the respective multiplets in 3–5 (Tables 1, S9, S10). This leads to higher spin reversal barriers in 4 and 6.^{3a}

The second reason is based on the direction of the anisotropy axes calculated for all complexes which are aligned in a parallel fashion due to the presence of an inversion center

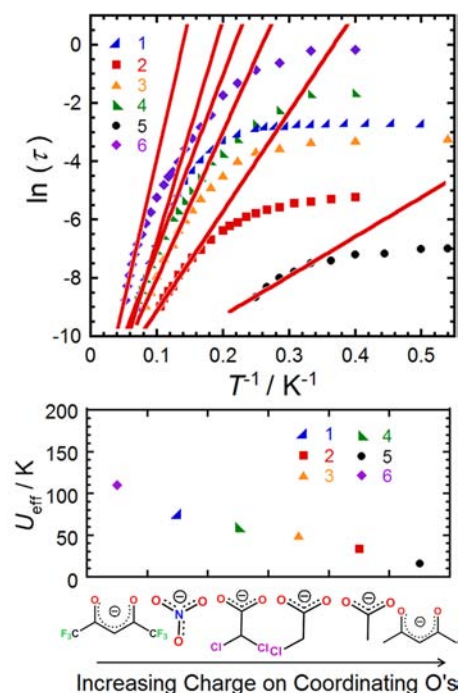


Figure 3. Top: Arrhenius plot showing the relaxation time of the magnetization for 1–6 under zero applied dc field. Red lines correspond to the fit of the high temperature data. Bottom: Plot of U_{eff} vs increasing charge on coordinating O's of the terminal ligands for 1–6.

Table 1. Energies (cm^{-1}) of the Low-Lying Kramers Doublets (KD) of the g Tensor in the Ground KD and the Main Values of the g Tensor in the Ground KD Obtained within Basis Set 2

J multiplet	2	3	4	5	6
	0	0	0	0	0
	132	148	155	22	182
	160	189	202	110	254
	206	264	280	132	312
$^6\text{H}_{15/2}$	252	289	341	179	359
	300	348	380	227	418
	349	402	446	265	465
	435	467	521	351	546
	Main Values of the g Tensor in the Ground KD				
g_x	0.027	0.0087	0.0041	0.091	0.00062
g_y	0.093	0.037	0.010	0.47	0.0033
g_z	19.44	19.50	19.50	18.87	19.66

(Figure S22). Furthermore, they are perpendicular to the capping ligand. The decreased electron density in the hard plane (perpendicular to the easy axis) could result in a more anisotropic Dy(III) ion leading to higher effective energy barriers. This was indeed observed when the calculated g tensors of the low-lying Kramers doublets (KD) of the Dy(III) ions were found to be more axial, and hence more anisotropic, for complexes 4 and 6 (Tables 1, S11, S12). Additionally, the low-lying exchange spectrum is shown in Table S13. Given the fact that the exchange splitting in these compounds is $< 3 \text{ cm}^{-1}$, we can conclude that the experimentally observed barriers originate from individual Dy(III) ions as seen for the parent compound, 1.^{5b} The discrepancies between extracted barriers and the calculated energies of the first excited KD of Dy(III)

ions can be attributed to room temperature geometry used in the calculations as well as the possibility that direct relaxation pathways should be considered.

In conclusion, we show significant enhancement of the energy barriers of two different systems of {Dy₂} SMMs by adding electron-withdrawing substituents on the terminal ligands in a systematic fashion. This resulted in a 2-fold increase in U_{eff} when dichloroacetate as opposed to acetate was employed and, more impressively, a 7-fold increase when the acac ligand was replaced by hexafluoroacac. The addition of electronegative atoms on the terminal ligands has been found to increase the Dy–Dy coupling with the static magnetic data being reproduced well using *ab initio* calculations. Furthermore, the *ab initio* calculations revealed more axial *g* tensors as well as first excited KDs that were highest in energy for complexes **4** and **6**, corresponding to higher energy barriers observed experimentally in their respective systems. Replacing H's with electron-withdrawing atoms on terminal ligands can be a relatively simple way of attaining higher barrier SMMs as opposed to the more synthetically challenging methods, such as inducing coupling of the metal centers using radical bridges or organometallic complexes. This methodology can provide a tool for future design of SMMs leading to potential applications in high-tech devices.

■ ASSOCIATED CONTENT

Supporting Information

Complete experimental, crystallographic, magnetic, and computational data for all complexes including CIF files. This material is available free of charge via the Internet at <http://pubs.acs.org>.

■ AUTHOR INFORMATION

Corresponding Author

m.murugesu@uottawa.ca

Notes

The authors declare no competing financial interest.

■ ACKNOWLEDGMENTS

We thank the University of Ottawa, NSERC and CIHR (Discovery and RTI grants, Vanier Graduate Scholarship) as well as CFI for their financial support.

■ REFERENCES

- (1) (a) Bogani, L.; Wernsdorfer, W. *Nat. Mater.* **2008**, *7*, 179. (b) Pfau, B.; Schaffert, S.; Müller, L.; Gutt, C.; Al-Shemmary, A.; Büttner, F.; Delaunay, R.; Düsterer, S.; Flewett, S.; Frömter, R.; Geilhufe, J.; Guehrs, E.; Günther, C. M.; Hawaldar, R.; Hille, M.; Jaouen, N.; Kobs, A.; Li, K.; Mohanty, J.; Redlin, H.; Schlotter, W. F.; Stickler, D.; Treusch, R.; Vodungbo, D.; Kläui, M.; Oepen, H. P.; Lüning, J.; Grübel, G.; Eisebitt, S. *Nat. Commun.* **2012**, *3*, 1100. (c) Rocha, A. R.; García-suárez, V. M.; Bailey, S. W.; Lambert, C. J.; Ferrer, J.; Sanvito, S. *Nat. Mater.* **2005**, *4*, 335.
- (2) (a) Neese, F.; Pantazis, D. A. *Faraday Discuss.* **2011**, *148*, 229. (b) Sessoli, R.; Powell, A. K. *Coord. Chem. Rev.* **2009**, *253*, 2328. (c) Habib, F.; Murugesu, M. *Chem. Soc. Rev.* **2013**, *42*, 3278. (d) Ishikawa, N.; Sugita, M.; Ishikawa, T.; Koshihara, S.-y.; Kaizu, Y. *J. Am. Chem. Soc.* **2003**, *125*, 8694. (e) Sorace, L.; Benelli, C.; Gatteschi, D. *Chem. Soc. Rev.* **2011**, *40*, 3092. (f) Woodruff, D. N.; Wimpenny, R. E. P.; Layfield, R. A. *Chem. Soc. Rev.* **2013**, *113*, 5110.
- (3) (a) Rinehart, J. D.; Long, J. R. *Chem. Sci.* **2011**, *2*, 2078. (b) Bernot, K.; Luzon, J.; Bogani, L.; Etienne, M.; Sangregorio, C.; Shanmugam, M.; Caneschi, A.; Sessoli, R.; Gatteschi, D. *J. Am. Chem.*

Soc. **2009**, *131*, 5573. (c) Ungur, L.; Chibotaru, L. F. *Phys. Chem. Chem. Phys.* **2011**, *13*, 20086.

(4) (a) Lin, P.-H.; Burchell, T. J.; Ungur, L.; Chibotaru, L. F.; Wernsdorfer, W.; Murugesu, M. *Angew. Chem., Int. Ed.* **2009**, *48*, 9489. (b) Watanabe, A.; Yamashita, A.; Nakano, M.; Yamamura, T.; Kajiwara, T. *Chem.—Eur. J.* **2011**, *17*, 7428. (c) Rinehart, J. D.; Fang, M.; Evans, W. J.; Long, J. R. *J. Am. Chem. Soc.* **2011**, *133*, 14236. (d) Rinehart, J. D.; Fang, M.; Evans, W. J.; Long, J. R. *Nat. Chem.* **2011**, *3*, 538. (e) Tuna, F.; Smith, C. A.; Bodensteiner, M.; Ungur, L.; Chibotaru, L. F.; McInnes, E. J. L.; Wimpenny, R. E. P.; Collison, D.; Layfield, R. A. *Angew. Chem., Int. Ed.* **2012**, *51*, 6976. (f) Blagg, R. J.; Tuna, F.; McInnes, E. J. L.; Wimpenny, R. E. P. *Chem. Commun.* **2011**, *47*, 10587.

(5) (a) Long, J.; Habib, F.; Lin, P.-H.; Korobkov, I.; Enright, G.; Ungur, L.; Wernsdorfer, W.; Chibotaru, L. F.; Murugesu, M. *J. Am. Chem. Soc.* **2011**, *133*, 5319. (b) Habib, F.; Lin, P.-H.; Long, J.; Korobkov, I.; Wernsdorfer, W.; Murugesu, M. *J. Am. Chem. Soc.* **2011**, *133*, 8830.

(6) (a) Cucinotta, G.; Perfetti, M.; Luzon, J.; Etienne, M.; Car, P.-E.; Caneschi, A.; Calvez, G.; Bernot, K.; Sessoli, R. *Angew. Chem., Int. Ed.* **2012**, *51*, 1606. (b) Martínez-Pérez, M. J.; Cardona-Serra, S.; Schlegel, C.; Moro, F.; Alonso, P. J.; Prima-García, H.; Clemente-Juan, J. M.; Evangelisti, M.; Gaita-Ariño, A.; Sesé, J.; van Slageren, J.; Coronado, E.; Luis, F. *Phys. Rev. Lett.* **2012**, *108*, 247213. (c) Habib, F.; Long, J.; Lin, P.-H.; Korobkov, I.; Ungur, L.; Wernsdorfer, W.; Chibotaru, L. F.; Murugesu, M. *Chem. Sci.* **2012**, *3*, 2158. (d) Williams, U. J.; Mahoney, B. D.; DeGregorio, P. T.; Carroll, P. J.; Nakamaru-Ogiso, E.; Kikkawa, J. M.; Schelter, E. J. *Chem Commun.* **2012**, *48*, 5593.

(7) Langley, S. K.; Chilton, N. F.; Moubaraki, B.; Murray, K. S. *Chem. Commun.* **2013**, *49*, 6965.

(8) (a) Chibotaru, L. F.; Ungur, L. *J. Chem. Phys.* **2012**, *137*, 064112. (b) Aquilante, F.; De Vico, L.; Ferre, N.; Ghigo, G.; Malmqvist, P.-A.; Neogrady, P.; Pedersen, T. B.; Pitonak, M.; Reiher, M.; Roos, B. O.; Serrano-Andres, L.; Urban, M.; Velyazov, V.; Lindh, R. *J. Comput. Chem.* **2010**, *31*, 224.

(9) (a) Brechin, E. K. *Chem. Commun.* **2005**, 5141. (b) Ferguson, A.; Lawrence, J.; Parkin, A.; Sanchez-Benitez, J.; Kamenev, K. V.; Brechin, E. K.; Wernsdorfer, W.; Hill, S.; Murrie, M. *Dalton Trans.* **2008**, 6409.

(10) Guo, Y.-N.; Xu, G.-F.; Gamez, P.; Zhao, L.; Lin, S.-Y.; Deng, R.; Tang, J.; Zhang, H.-J. *J. Am. Chem. Soc.* **2010**, *132*, 8538.

(11) (a) Cole, K. S.; Cole, R. H. *J. Chem. Soc.* **1941**, *9*, 341. (b) Aubin, S. M. J.; Sun, Z.; Pardi, L.; Krzystek, J.; Folting, K.; Brunel, L. J.; Rheingold, A. L.; Christou, G.; Hendrickson, D. N. *Inorg. Chem.* **1999**, *38*, 5329.

(12) Seitz, M.; Oliver, A. G.; Raymond, K. N. *J. Am. Chem. Soc.* **2007**, *129*, 11153.

(13) Trzesowska, A.; Kruszynski, R.; Bartczak, T. J. *Acta Crystallogr.* **2004**, *B60*, 174.